BMC Pharmacology and Toxicology

RESEARCH

Open Access

Therapeutic role of melatonin on acrylamide-induced neurotoxicity via reducing ER stress, inflammation, and apoptosis in a rat model

Yusuf Dag[1], Serkan Yildirim[2,3], Emin Sengul[1,4], Furkan Aykurt[1], Melahat Gok[1] and Ali Cinar[1*]

Abstract

This study examined the antioxidant, anti-inflammatory, and neuroprotective effects of melatonin (MEL) against acrylamide (ACR)-induced neurotoxicity in Sprague-Dawley rats. The experimental groups included control, ACR, MEL10+ACR, MEL20+ACR, and MEL20. MEL at doses of 10 and 20 mg/kg, and ACR at 50 mg/kg, were administered intraperitoneally for 14 days. On the 15th day, locomotor activity was assessed, and brain tissues were analyzed biochemically, molecularly, and histopathologically. ACR exposure decreased locomotor activity, increased malondialdehyde (MDA) and reduced glutathione (GSH) levels, indicating oxidative stress, and decreased antioxidant enzyme activities (SOD, GPx, CAT). High-dose MEL (MEL20+ACR) effectively reduced lipid peroxidation and restored antioxidant enzyme activities. MEL treatment also suppressed proinflammatory cytokines (TNF-α, IL-1β, IL-6) and neuronal nitric oxide synthase (nNOS), demonstrating anti-inflammatory effects. Furthermore, MEL mitigated ACR-induced neurotoxicity by reducing acetylcholinesterase (AChE) and monoamine oxidase (MAO) levels. ER stress markers (GRP78, ATF4, ATF6, sXBP1, CHOP) and apoptotic markers (Bax, Caspase-3) were elevated following ACR exposure but were suppressed by MEL. Additionally, MEL reduced ACR-induced increases in 8-hydroxy-2-deoxyguanosine (8-OHdG) and glial fibrillary acidic protein (GFAP), markers of DNA damage and astrocyte activation, respectively. These findings underscore the potential of MEL to counteract ACR-induced neurotoxicity through its comprehensive antioxidant, anti-inflammatory, and neuroprotective actions.

*Correspondence:
Ali Cinar
d.cinar@atauni.edu.tr

Full list of author information is available at the end of the article

Graphical abstract

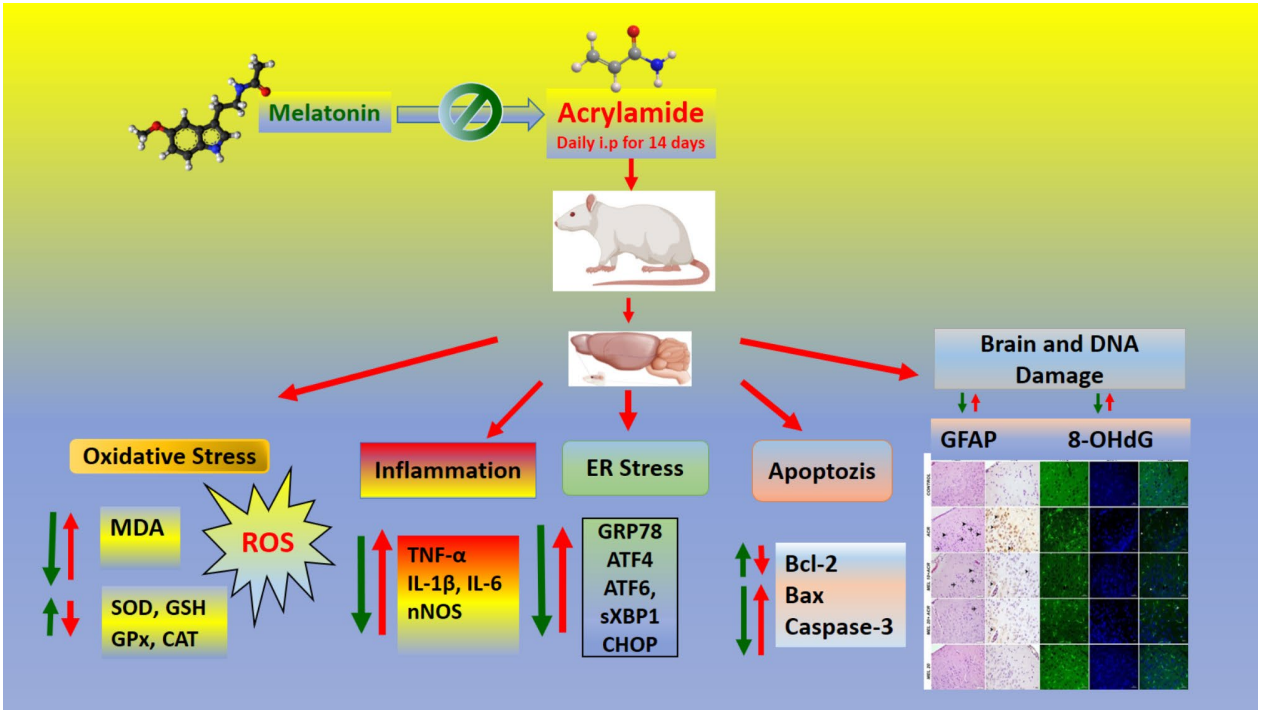

Keywords Acrylamide, Apoptosis, Endoplasmic reticulum stress, Locomotor activity, Melatonin

Introduction

Acrylamide (ACR) is a neurotoxic compound generated during high-temperature processing of tobacco and carbohydrate-rich foods and is a substantial public health concern due to frequent exposure in daily life. Commonly employed in various industrial sectors, such as construction and manufacturing, ACR exposure is prevalent among workers, posing potential risks of contamination in food sources [1, 2]. Previous studies have shown that ACR is formed when carbohydrate-rich foods are exposed to temperatures exceeding 120 °C. ACR exposure primarily occurs through skin contact, inhalation, and ingestion. Additionally, it can traverse the placental barrier, potentially inducing fetal anomalies [3, 4]. ACR is recognized as a carcinogen capable of inducing breast [5], kidney [6], bladder, and prostate [7] cancers when ingested with food. Furthermore, it exerts toxic effects on kidney [8–10], reproductive organs [11] and induces neuropathy [12]. The ability of ACR to permeate the blood–brain barrier leads to elevated oxidative stress in brain tissues, culminating in neurotoxicity [13].

Neurodegeneration as a result of the toxic impact on brain tissue triggers the release of proinflammatory mediators through the activation of reactive oxygen species (ROS) and cytokines. ACR-induced neurotoxicity arises from both chemical and biochemical effects. Despite extensive investigations into its underlying mechanisms, the intracellular stress signaling pathways involved in ACR-induced neurotoxicity are incompletely understood [14, 15]. One key factor in this process is the endoplasmic reticulum (ER), which plays a pivotal role in neural plasticity. The ER regulates essential biological processes such as protein synthesis, folding, and post-translational modification. When neuronal cells encounter extracellular stressors, unfolded proteins accumulate within the ER lumen, leading to ER stress. This accumulation triggers an adaptive response known as the unfolded protein response (UPR), aimed at alleviating stress [16]. However, if the UPR fails to resolve the excessive buildup of unfolded proteins, it activates signaling pathways that promote inflammation and apoptosis, potentially leading to neurodegenerative disorders. ER stress is significant in diseases such as Alzheimer's disease, Parkinson's disease, amyotrophic lateral sclerosis, polyglutamine diseases, ischemia, atherosclerosis, bipolar disorder, prion diseases, cancer, diabetes, and autoimmune and cardiovascular disorders [17]. Moreover, neurotoxic agents, chemotherapeutic drugs, and various chemical compounds present in food can induce ER stress, provoking oxidative stress and subsequent neurotoxicity [18]. This reciprocal relationship between oxidative stress and ER stress exacerbates inflammation and promotes neuronal

apoptosis [18–20]. ACR is implicated in inflammation and apoptosis via the induction of ER stress. Previous studies have shown that ACR triggers neuronal ER stress, neuroinflammation, and neuronal apoptosis [21]. Protective strategies against ACR-induced neurotoxicity often involve antioxidant and anti-inflammatory compounds [22].

Melatonin (MEL), a hormone with immunostimulatory and cytoprotective properties, has garnered increasing attention for its potential neuroprotective effects [23]. It regulates immune function and exhibits antioxidant and anti-inflammatory properties and has been reported to mitigate oxidative stress-induced neuronal apoptosis and degeneration [24]. MEL is gaining attention for its neuroprotective effects by reducing oxidative stress-induced neuronal apoptosis and degeneration. Recent studies have shown its ability to modulate ER stress and ameliorate neurodegeneration [23, 25].

Furthermore, recent studies have shown that MEL can modulate neurodegenerative diseases by regulating ER stress. For instance, studies have demonstrated that MEL is neuroprotective effects against ACR-induced brain damage in pinealectomized rats [26]. Additionally, research has highlighted the therapeutic role of MEL on ACR-induced hepatotoxicity, showing its effects on oxidative stress, NF-κB signaling pathway, and hepatocellular proliferation [27]. Furthermore, MEL has been shown to attenuate oxidative damage induced by ACR in vitro and in vivo [28].

While there is substantial research on the neuroprotective effects of MEL against ACR-induced neurotoxicity in various contexts, the novelty of this study lies in its detailed exploration of effects of MEL on ER stress, neuroinflammation, and neuronal apoptosis specifically within ACR-exposed rat brain tissues. Unlike previous studies that focused on individual aspects such as brain damage, hepatotoxicity, or oxidative stress, this research delves into the comprehensive mechanisms by which MEL mitigates these interconnected processes. This study aims to fill the existing research gap by elucidating role of MEL in modulating ER stress-related pathways and reducing neuroinflammation and apoptosis, providing new insights into its therapeutic potential against ACR-induced neurotoxicity in the brain.

Materials and methods

Animals and experimental design

The research was approved by the Atatürk University Ethical Committee for laboratory animal experiments (Ethics Committee Protocol number: 2020/41). All experiments were performed in strict accordance with the ARRIVE guidelines and all relevant institutional and national regulations for the care and use of laboratory animals. Fifty healthy male adult Sprague Dawley rats, aged 12 weeks and weighing 220–250 g, were obtained from the Atatürk University Experimental Animals Research and Application Center. Additionally, all methods were carried out in compliance with the guidelines and regulations specified by the Biomed Central ethical policies.

Rats were randomly divided into five experimental groups: control, ACR, MEL10+ACR, MEl20+ACR and MEL20. ACR (50 mg/kg [8], intraperitoneally (i.p.), 14 days) and two different doses of MEL (10 and 20 mg/kg, i.p., 14 days) [8] were administered to the experimental groups. Before use in any of the experiments described here, the experimental animals were adapted to the laboratory setting for one week and fed ad libitum while being kept under suitable conditions. The control group was subjected to i.p. injection for 14 days. One milliliter (mL) of saline or ACR (50 mg/kg, i.p.) was administered to the rats in the ACR group for 14 days. The MEL10+ACR and MEL20+ACR groups were given i.p. doses of 10 and 20 mg/kg, respectively, for 14 days. MEL was administered, and ACR (50 mg/kg, i.p.) was injected 1 h after each MEL application. In the MEL20 group, MEL was administered at a dose of 20 mg/kg (i.p.) for 14 days.

Locomotor activity test

Plexiglass cages ($42 \times 42 \times 42$ cm^3) were used for the LMA test measurements in experimental animals. The stereotypic, ambulatory, horizontal, vertical and distance activities of the rats were measured. After the rats were injected, each rat was placed in the middle of the cage, and all parameters were recorded for 10 min. Silence was maintained throughout the testing period while the recording was being made. After each rat measurement, the cages were cleaned with 30% ethanol to prevent any odors from remaining. In this way, increases or decreases in the LMA activities of rats were detected in the study [29].

At the end of the LMA test, the live weight of the rats was measured. After that all rats were anesthetized using %3 sevoflurane inhalation anesthesia (Sevorane liquid, AbbVie Laboratories, Istanbul, Turkey) for 3 min, which is enough for complete loss of sensation [30]. Then animals were decapitated and their brain tissues were collected. Half of the brain tissue was immediately frozen in liquid nitrogen after being washed with physiological saline, and the other half was placed in 10% formaldehyde for histopathological and immunohistochemical examinations.

Biochemical analysis

Brain tissue samples were homogenized using a Magna Lyser homogenizer (Roche) at 6000 rpm for 90 s, followed by centrifugation to collect the supernatant.

The concentrations of various parameters, including MDA, SOD, GPx, GSH, CAT, TNF-α, IL-6, IL-1β, nNOS, AChE, and MAO, were measured in the brain tissue supernatants using commercially available ELISA kits designed for rats (Sunred Biological Technology, Shanghai, China) following the manufacturer's instructions. Plate readings were obtained using a BioTek ELISA reader equipped with the EPOCH II program at a wavelength of 450 nm, and the results were compared between the experimental groups.

Assessment of gene expression levels via real-time PCR

To measure the expression levels of the gene regions determined in this study, total RNA isolation, cDNA synthesis and amplification by PCR were first performed.

Total RNA isolation

The expression levels of the GRP78, ATF4, ATF6, sXBP-1, CHOP, Bax, Bcl-2, and Caspase-3 genes, along with the housekeeping gene GAPDH mRNA, were quantified in brain tissues using real-time PCR and compared between the experimental groups. Total RNA extraction was performed to isolate RNA from the tissues. Total RNA isolation was carried out using an Omega RNA-Solv Reagent kit (BIO-TEK, LOT: R6830118886-33, USA) following the manufacturer's protocol.

cDNA synthesis

A High Capacity cDNA Reverse Transcription Kit from Applied Biosystems was utilized for cDNA synthesis from total RNA samples. A total reaction volume of 20 µl was prepared, comprising reverse transcriptase enzyme, dNTPs, and template RNA. Specifically, 2.0 µl of 10X RT Buffer, 0.8 µl of 25X dNTP Mix (100 mM), 2.0 µl of 10X RT Random Primers, 1.0 µl of MultiScribe Reverse Transcriptase, and 4.2 µl of nuclease-free H2O were combined with 10 µl of template RNA.

cDNA synthesis was performed using the thermocycler was used under the following specified conditions: initial primer annealing step at 25 °C for 10 min, followed by a reverse transcription extension step at 37 °C for 120 min, a reverse transcriptase enzyme inactivation step at 85 °C for 5 min, and a final cooling step at 4 °C. Following synthesis, cDNA concentrations were measured, and the samples were stored at -20 °C until further analysis via real-time PCR.

The expression levels of different genes by real-time PCR

The primers used for quantifying mRNA transcript levels via real-time PCR were designed using the Primer Design tool available at the following link (https://www.ncbi.nlm.nih.gov/tools/primer-blast/), as outlined in Table 1.

The requisite storage reagents, comprising SYBR Green master mix, cDNA, primers, and nuclease-free water, were used for defrosting, followed by thawing and equilibration to 5 °C. Subsequently, a master mix was prepared by combining 10 µl of SYBR Green master mix, 1.5 µl each of forward and reverse primers, 5 µl of nuclease-free water, and 2 µl of cDNA per reaction, adhering to the protocol outlined in the Sybr Green 2X Rox Dye Master Mix (Qiagen). All work was performed on a cold block to maintain the integrity of the reagents.

Real-time PCR was conducted using a thermocycler. The samples were programmed with an initial denaturation step of 15 min at 95 °C, followed by 40 cycles of denaturation at 94 °C for 15 s, annealing at 60 °C for 20 s, and extension at 72 °C for 20 s. Subsequently, the samples were indefinitely preserved at 4 °C before further analysis. The resulting Ct/Cq values were analyzed using the $2^{-\Delta\Delta CT}$ method to quantify the expression levels of the target genes.

Table 1 Primers used in real-time PCR experiments

GENE	Sequence (5′ – 3′)	Base length	Accession number
GRP78	F: CGCCTGACCCCTGAAGAAAT R: TGGCTTTCCAGCCATTCGAT	230	S63521.1
ATF4	F: TATCTGGAGGTGGCCAAGCA R: CTCCAACATCCAATCTGTCC	147	NM_024403.2
ATF6	F: TCCTCATGGACCAGGTGAAGAC R: AGTCCAACTCCTCAGGAACG	305	NM_001107196.1
sXBP1	F: GCTGCGGAGGAAACTGAAAAA R: CACGTAGTCTGAGTGCTGCG	299	NM_001004210.2
CHOP	F: TGTTGAAGATGAGCGGGTGG R: CCGGTTTCTGCTTTCAGGTG	117	NM_001109986.1
Bax	F: ACACCTGAGCTGACCTTGGA R: AGTTCATCGCCAATTCGCCT	86	NM_017059.2
Bcl-2	F: CTGGTGGACAACATCGCTCT R: GCATGCTGGGGCCATATAGT	115	NM_016993.1
Caspase-3	F: GGAGCTTGGAACGCGAAGAA R: ACACAAGCCCATTTCAGGGT	169	NM_012922.2
GAPDH	F: AGTGCCAGCCTCGTCTCATA R: GATGGTGATGGGTTTCCCGT	248	NM_017008.4

Histopathological examinations

Upon completion of the assessment, brain tissue specimens retrieved from the rats were fixed in a 10% formalin solution for 48 h following a standard tissue processing protocol. Subsequently, the tissues were stained with hematoxylin-eosin (HE) and analyzed using a light microscope (Olympus BX 51, Japan). The histopathological characteristics of the sections were graded according to the severity of their morphological features and categorized as absent (-), mild (+), moderate (++), or severe (+++).

Immunohistochemical examination

Following the deparaffinization and dehydration of brain tissue sections, a primary antibody against 8-oxo-2'-deoxyguanosine (8-OHdG; Cat No: sc-66036, dilution ratio; 1/100 US) was applied using standard procedures, and the sections were then incubated at 37 °C for 1 h. Subsequently, 3–3'-diaminobenzidine (DAB) was added to the sections. The stained sections were examined using a light microscope (Zeiss AXIO).

Immunofluorescence examination

Following the deparaffinization and dehydration of brain tissue sections, a primary antibody against Glial Fibrillary Acidic Protein (GFAP; Cat No: sc-33673, dilution ratio: 1/200) was applied following standard procedures, and the tissues were incubated according to the kit instructions. Subsequently, an immunofluorescence secondary antibody (FITC Cat No: ab6717, dilution ratio: 1/1000) was applied, and the samples were incubated for 45 min in the dark. Next, the DNA marker DAPI (Cat No: D 1306, dilution ratio: 1/200 UK) was added, and the samples were incubated in the dark for 5 min. Then, the tissues were examined under a fluorescence microscope (Zeiss AXIO).

Statistical analysis

The quantitative data of the obtained results were statistically analyzed using the Tukey test following one-way ANOVA, which is employed for statistical analysis involving more than two independent groups. The analysis was conducted using GraphPad Prism 8.0.1 statistical software. The significance level of alpha (α) was set at $P < 0.05$.

Results

Effects of ACR and MEL on body and brain weights

Table 2 provides a summary of the initial and final body and brain weights. Initially, there were no significant differences in the live weights of the rats across the groups ($p > 0.05$). However, upon concluding the experimental study, it became evident that the average live weights of rats in the ACR and MEL10+ACR groups were notably lower than those in the other groups ($p < 0.05$).

Effects of ACR and MEL on locomotor activity

Figures 1 and 2 depict the outcomes of the locomotor activity test, revealing notable alterations in rat movement and behavior following ACR-induced neurotoxicity. Analysis revealed a significant decrease in stereotypic, ambulatory, distance, and horizontal movements in the ACR and MEL10+ACR groups compared to the other groups. Specifically, rats treated with ACR alone exhibited reduced locomotor activities, indicating the neurotoxic effects of ACR. The reduction in movements is indicative of impaired motor functions and neurobehavioral deficits. In contrast, the MEL20+ACR and MEL20 groups did not show significant differences from the control group ($p > 0.05$), suggesting a protective effect of MEL at higher doses. This observation implies that MEL, particularly at a dose of 20 mg/kg, effectively mitigates the neurotoxic effects of ACR, preserving normal locomotor activities in rats. Moreover, vertical movements were significantly lower in the ACR, MEL10+ACR, and MEL20+ACR groups than in the control and/or MEL20 groups ($p < 0.0001$). This reduction in vertical movements further supports the observation that ACR induces neurotoxicity, affecting not only horizontal locomotion but also the exploratory behavior of the rats. Additionally, the MEL10+ACR group showed a partial improvement in locomotor activities compared to the ACR group, indicating a dose-dependent protective effect of MEL. While the lower dose of MEL (10 mg/kg) provided some neuroprotective benefits, it was not as effective as the higher dose (20 mg/kg) in reversing the ACR-induced deficits in locomotor activity. These findings highlight the potential therapeutic role of MEL in mitigating ACR-induced neurotoxicity, with higher doses offering more substantial protection. The data underscore the importance of dose optimization in the use of MEL as a neuroprotective agent against environmental neurotoxins like ACR.

Table 2 Body and brain weights of rats in the experimental groups ($n = 10$)

Parameters	Control	ACR	MEL10+ACR	MEL20+ACR	MEL20
Initial body weights (g)	214,25 ± 12,08[a]	216.03 ± 9.93[a]	215.25 ± 9.60[a]	216.02 ± 9.53[a]	214.50 ± 11.19[a]
Final body weights (g)	255.12 ± 9.40[a]	192.75 ± 14.33[b]	195.37 ± 14.91[b]	240.12 ± 11.65[a]	254.25 ± 10.05[a]
Brain weights (g)	1.8295 ± 0.024[a]	1.8067 ± 0.050[a]	1.8055 ± 0.048[a]	1.802 ± 0.042[a]	1.8331 ± 0,052[a]

Statistical significance between groups within each row is denoted by different letters (a, b, c). Values are reported as mean ± SEM (Standard Error of the Mean). Groups marked with different letters show significant differences (a-b: $p < 0.05$; $n = 10$)

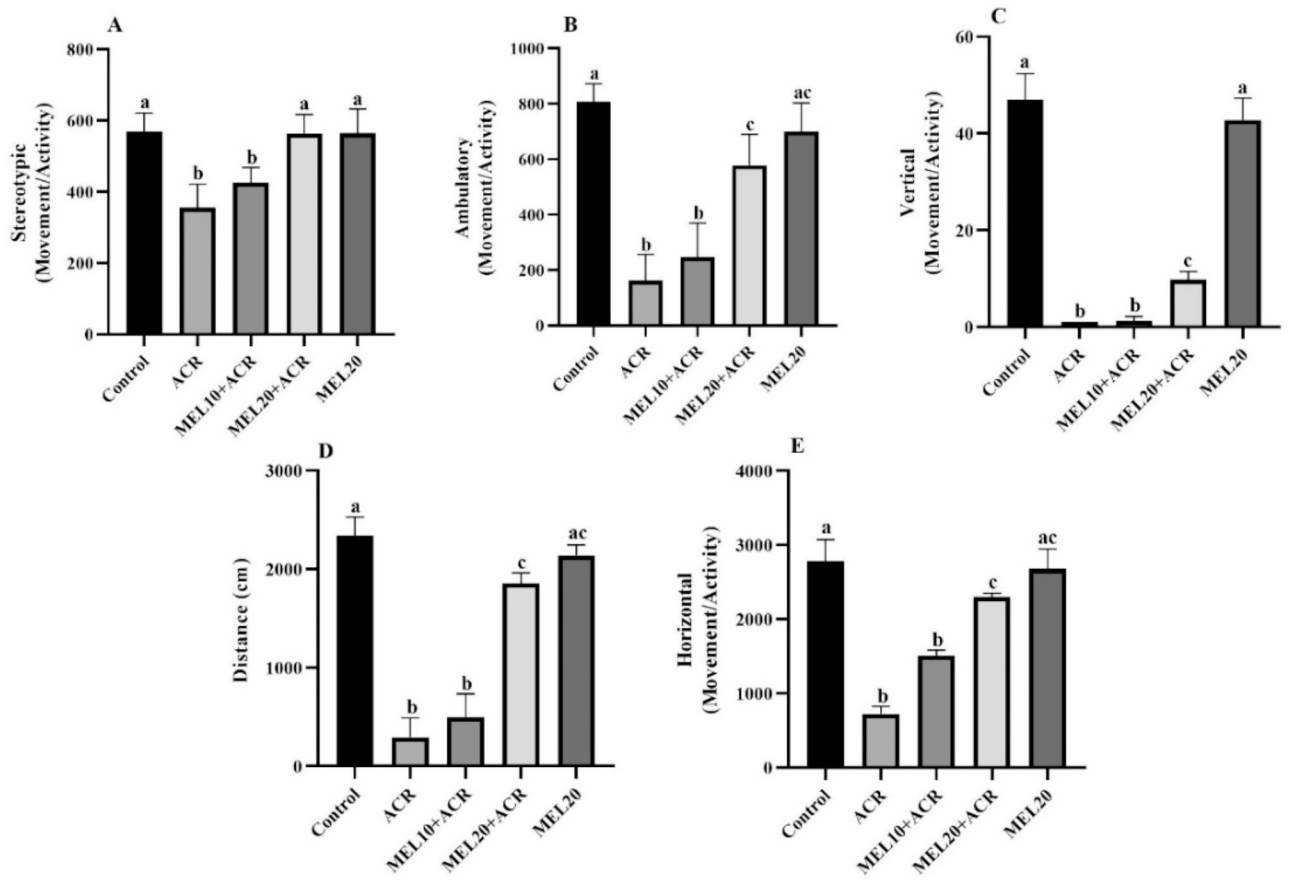

Fig. 1 Effects of MEL on locomotor activity parameters in ACR-induced neurotoxicity. The letters (a, b, c) indicate significant differences between columns ($p < 0.05$; $n = 10$). The error bars represent the standard error of the Mean (SEM)

Effects of ACR and MEL on MDA and GSH levels and SOD, GPx and CAT activities in brain tissues

As presented in Table 3, the level of the lipid peroxidation parameter MDA in brain tissue was significantly greater in the ACR and MEL10+ACR groups than in the other groups ($p < 0.0001$). However, MEL treatment effectively mitigated this elevation in a dose-dependent manner ($p < 0.05$), with MDA levels in the MEL20+ACR and MEL20 groups similar to those in the control group ($p > 0.05$). Conversely, the GSH level was significantly lower in the ACR and MEL10+ACR groups than in the other groups ($p < 0.0001$). Treatment with MEL reversed this reduction in a dose-dependent manner, with GSH levels in the MEL20+ACR and MEL20 groups comparable to those in the control group.

The antioxidant enzyme activities of SOD, GPx, and CAT in the brain tissues of the rats were notably lower in the ACR and MEL10+ACR groups than in the other experimental groups. However, MEL treatment effectively counteracted this reduction in enzyme activity in a dose-dependent manner. Specifically, the activities of these enzymes in the MEL20+ACR and MEL20 groups were comparable to those observed in the control group ($p > 0.05$).

Effects of ACR and MEL on TNF-α, IL-1β, IL-6 and nNOS levels

Table 3 show significant elevations in the levels of the proinflammatory mediators TNF-α, IL-1β, IL-6 and nNOS in the brain tissues of the rats in the ACR and MEL10+ACR groups compared with those in the control and other groups. Notably, both doses of MEL mitigated the ACR-induced increase in these parameters in a dose-dependent manner.

Effects of ACR and MEL on ache and MAO levels

As shown in Table 3, the activities of the neuromodulatory enzymes AChE and MAO in the rat brain were notably elevated in the ACR group compared to the other groups ($p < 0.0001$). However, the administration of two doses of MEL effectively mitigated this elevation in enzyme levels.

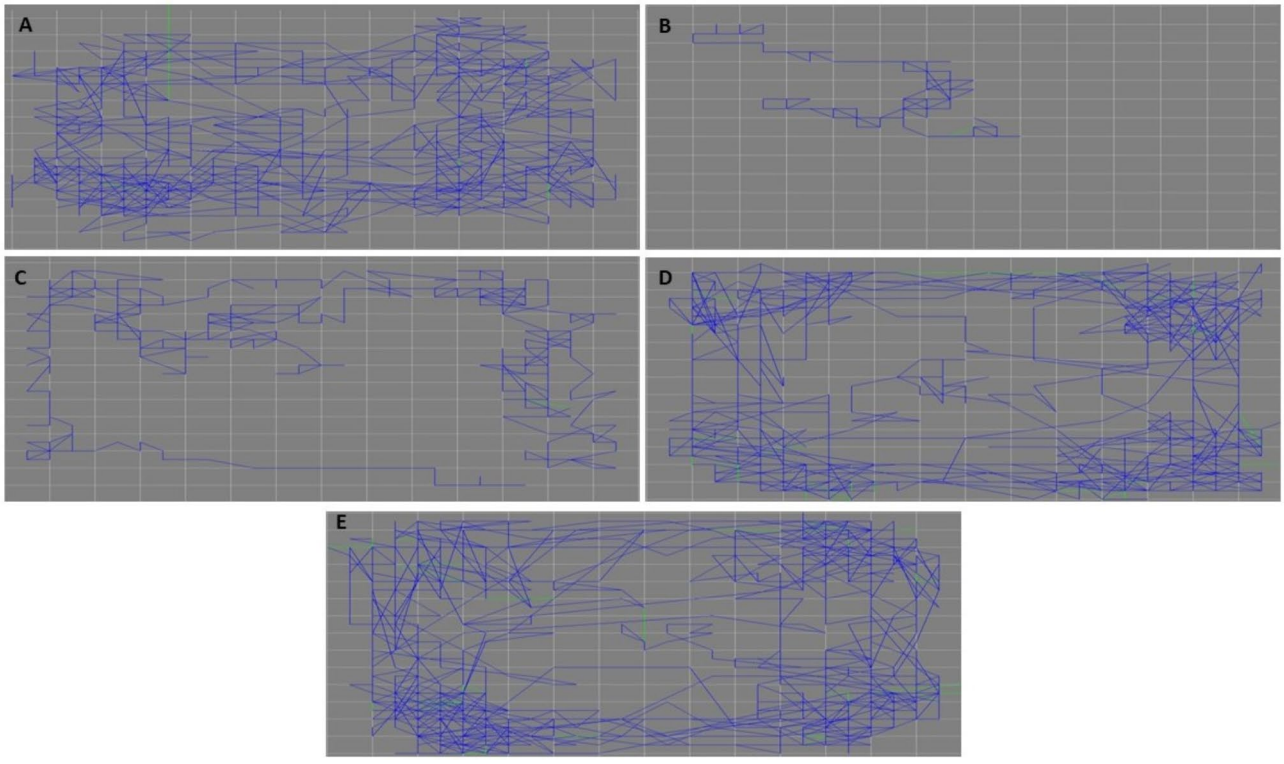

Fig. 2 Representative effects of ACR-induced neurotoxicity on locomotor activity parameters in the open field test (**A**: Control, **B**: ACR, **C**: MEL10+ACR, **D**: MEL20+ACR, and **E**: MEL20)

Table 3 Biochemical parameters in different experimental groups ($n = 10$)

Parameters	Experimental groups				
	Control	ACR	MEL10+ACR	MEL20+ACR	MEL20
MDA (nmol/mg)	3.49 ± 0.41a	5.87 ± 0.63^{b}	4.97 ± 0.39^{b}	4.12 ± 0.21^{c}	3,89 ± 0,39^{ac}
SOD (U/mg)	7.11 ± 0.21a	6.08 ± 0.23^{b}	6.50 ± 0.14^{c}	6.90 ± 0.11^{a}	6.90 ± 0.19 ^{a}
GSH (µmol/g)	0.445 ± 0.031a	0.314 ± 0.025b	0.376 ± 0.015c	0.423 ± 0.020a	0.436 ± 0.029a
GPx (U/mg)	12.30 ± 0.38a	8.30 ± 0.79^{b}	9.45 ± 0.87^{b}	11.30 ± 0.56^{c}	11.91 ± 0.48^{ac}
CAT (U/mg)	20.73 ± 1.02a	15.05 ± 0.43^{b}	16.68 ± 1.16^{b}	19.72 ± 1.23^{a}	20.58 ± 0.98^{a}
TNF-α (ng/L)	73.56 ± 2.46^{a}	90.54 ± 3.44^{b}	84.57 ± 1.99^{c}	76.01 ± 2.33^{a}	74.43 ± 1.45^{a}
IL-1β (pg/L)	405.31 ± 21.20^{a}	491.15 ± 22.96^{b}	448.48 ± 19.43^{c}	415.44 ± 17.24^{ac}	409.91 ± 16.11^{a}
IL-6 (pg/ml)	34.76 ± 1.90^{a}	46.84 ± 2.88^{b}	43.35 ± 1.96^{b}	37.69 ± 2.40^{a}	36.26 ± 2.31^{a}
nNOS (ng/ml)	8.80 ± 0.73^{a}	14.10 ± 1.06^{b}	10.79 ± 1.33^{c}	9.45 ± 0.66^{ac}	9.29 ± 0.64^{ac}
AChE (ng/ml)	7.68 ± 0.78^{a}	10.30 ± 0.64^{b}	8.68 ± 1.00^{a}	7.95 ± 0.75^{a}	7.76 ± 0.83^{a}
MAO (nmol/min/mg)	1.85 ± 0.13^{a}	3.03 ± 0.30^{bc}	2.44 ± 0.31^{c}	2.07 ± 0.24^{ac}	2.01 ± 0.24^{ac}

Statistical significance between groups within each row is denoted by different letters (a, b, c). Values are reported as mean ± SEM (Standard Error of the Mean). Groups marked with different letters show significant differences (a-b: $p < 0.01$; a-c: $p < 0.05$, $n = 10$)

Effects of ACR and MEL on GRP78, ATF4, ATF6, sXBP1 and CHOP gene expression

The expression levels of the GRP78, ATF4, ATF6, sXBP1, and CHOP genes in brain tissues (Fig. 3) were significantly greater in the ACR group than in the other groups. Notably, the administration of both low and high doses of MEL effectively attenuated these increases. Although the gene expression levels of GRP78, ATF4, ATF6, sXBP1, and CHOP were greater in the MEL10+ACR group than in the control group, the analysis revealed no discernible difference in these values between the MEL20+ACR group and the control group.

Effects of ACR and MEL on Bax, Bcl-2 and Caspase-3 gene expression levels

ACR-induced neuronal apoptosis was evidenced by a marked increase in the levels of the proapoptotic proteins Bax and Caspase-3 in the brain tissue of the ACR and MEL10+ACR groups compared to the other groups.

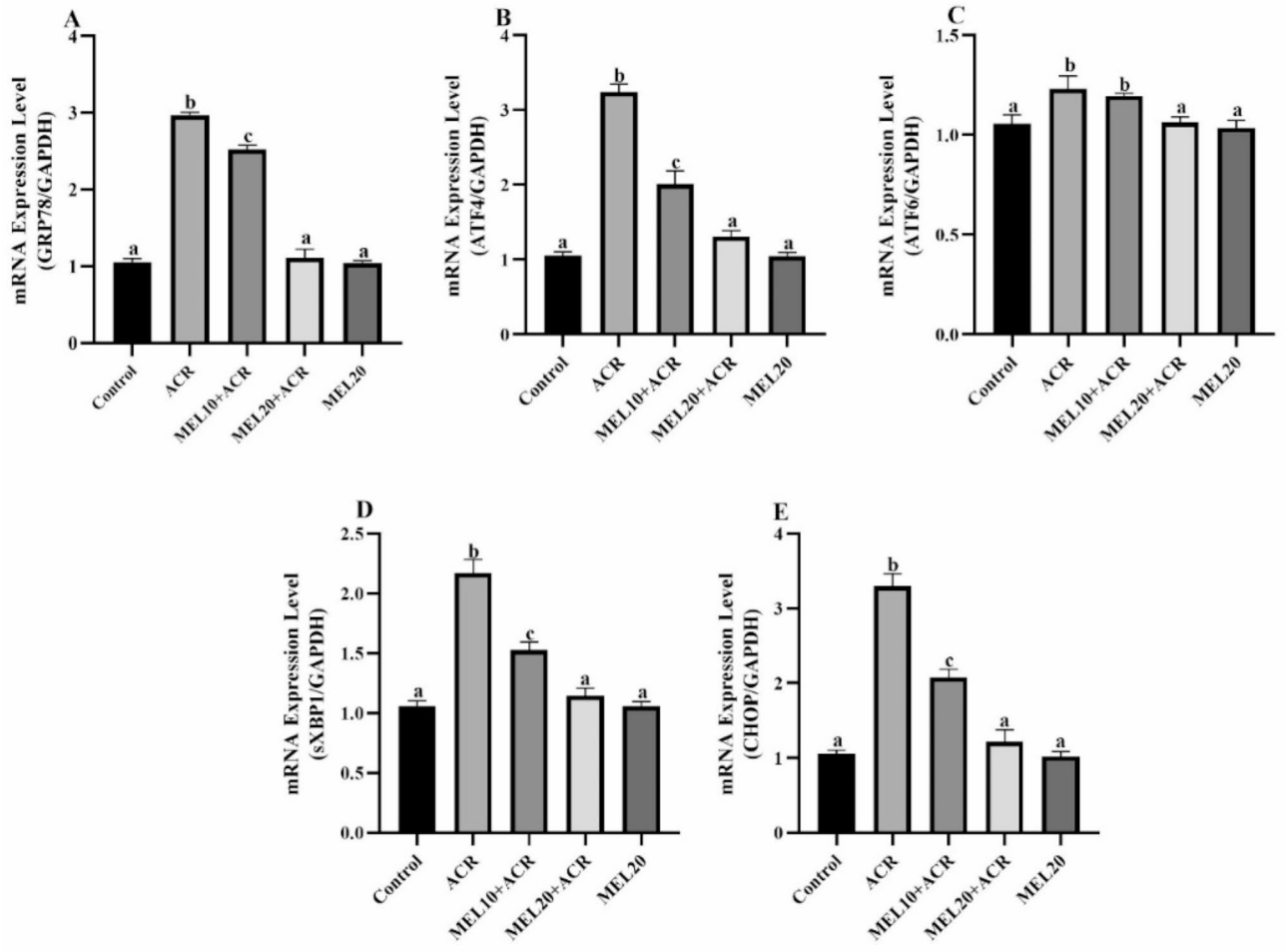

Fig. 3 Effects of MEL and ACR on the levels of GRP78 (**A**), ATF4 (**B**), ATF6 (**C**), sXBP1 (**D**) and CHOP (**E**) gene expression in the brain tissues of rats. The letters (a, b, c) indicate significant differences between columns ($p < 0.05$; $n = 10$). The error bars represent the Standard Error of the Mean (SEM)

Both doses of MEL were observed to exacerbate these parameters in a dose-dependent manner. Additionally, the level of the antiapoptotic protein Bcl-2 was markedly lower in the ACR and MEL10+ACR groups than in the other groups (Fig. 4).

Effects of ACR and MEL on brain tissue histopathology

Histopathological examination of the rat brain at the end of the experiment revealed distinct findings across the experimental groups. The control and MEL20 groups exhibited normal histological features, while the ACR group displayed severe neuronal degeneration and necrosis, as well as pronounced hyperemia in the meningeal and parenchymal vessels. The MEL10+ACR group exhibited moderate neuronal degeneration, mild necrosis, and severe hyperemia, while the MEL20+ACR group exhibited mild neuronal degeneration and vessel hyperemia. The detailed histopathological findings are summarized in Table 4.

Effects of ACR and MEL on 8-OHdG expression in brain tissue

The expression of 8-OHdG in brain tissues, with negative scores observed in the control and MEL20 groups. Conversely, the ACR group exhibited severe cytoplasmic 8-OHdG expression. In the MEL10+ACR group, moderate levels of 8-OHdG expression were detected in neurons, while the MEL20+ACR group displayed mild cytoplasmic 8-OHdG expression. The detailed immunohistochemical findings are also provided in Table 5; Fig. 5.

Effects of ACR and MEL on GFAP expression in brain tissue

GFAP expression in the brain tissues of the control and MEL20 groups was evaluated as negative. Severe GFAP expression was detected in astrocytes in the brain tissues of the ACR group, and moderate GFAP expression was detected in the brain tissues of the MEL10+ACR group. GFAP expression was detected at a mild level in astrocytes in the MEL20+ACR group. The immunofluorescence results are summarized in Table 5; Fig. 5.

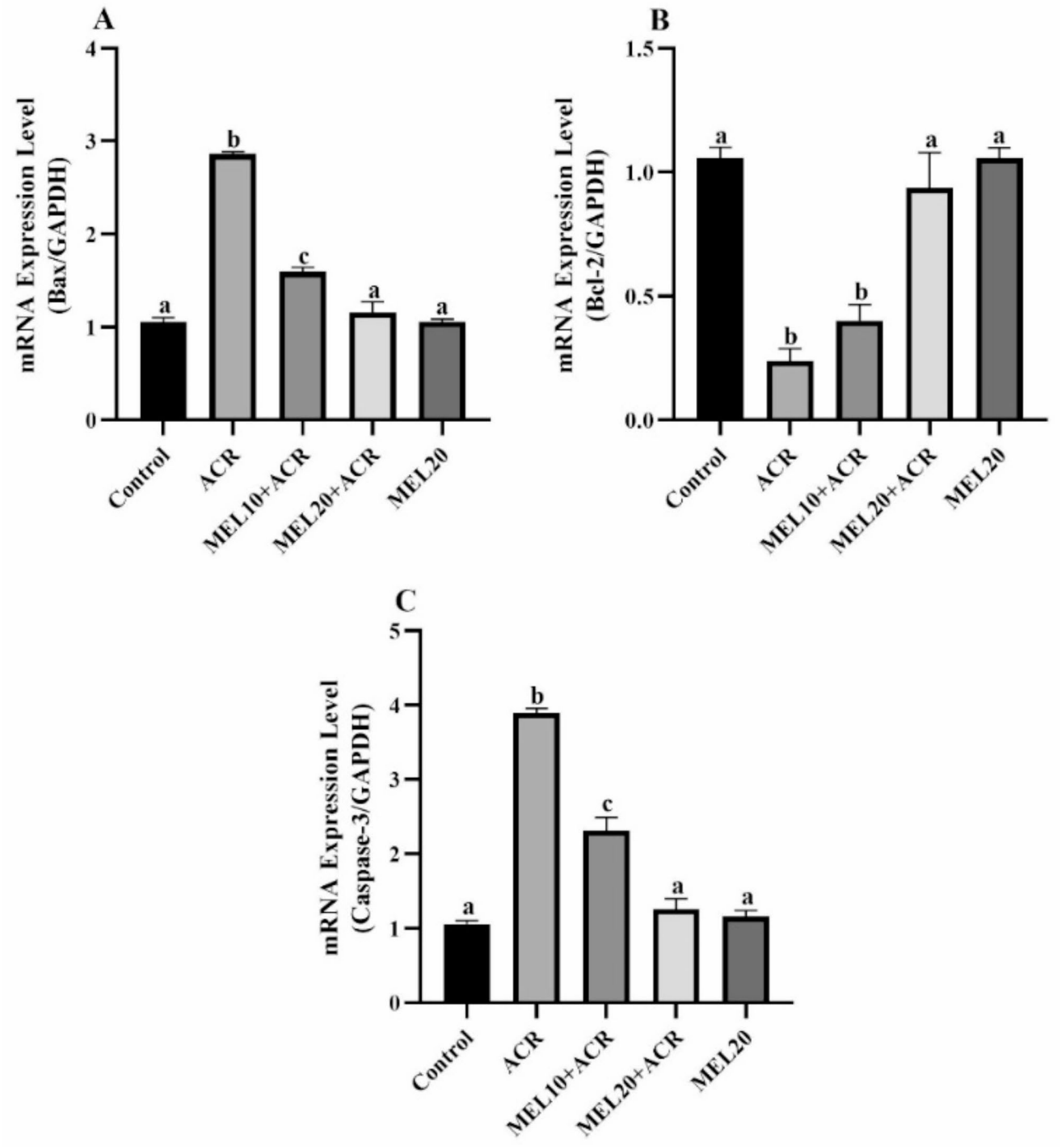

Fig. 4 Effects of MEL and ACR on the levels of Bax (**A**), Bcl-2 (**B**) and Caspase-3 (**C**) gene expression in the brain tissues of rats. The letters (a, b, c) indicate significant differences between columns ($p < 0.05$; $n = 10$). The error bars represent the Standard Error of the Mean (SEM)

Discussion

ACR is a hydrophilic compound with a low molecular weight facilitating its extensive tissue penetration. Various studies have underscored its extensive toxicity spectrum, encompassing neurotoxicity, genotoxicity, carcinogenicity, reproductive toxicity, and ecotoxicity. The Environmental Scientific Committee also emphasized these concerns. The biotransformation of ACR primarily occurs through cytochrome P450 2E1 (CYP2E1), resulting in the formation of glycidamide metabolites that are known to induce damage to both DNA and proteins [31]. Its toxicity typically starts with hind limb paralysis, along with weight loss [10]. In our study, neurotoxicity was

Table 4 Histopathological findings in the brain tissues of the experimental groups

Results	Control	ACR	MEL10+ACR	MEL20+ACR	MEL20
Neuronal Degeneration	-	+++	++	+	-
Neuronal Necrosis	-	+++	+	-	-
Vascular Hyperemia	-	+++	+++	++	-

Table 5 Analysis of data of immunohistochemical and immunofluorescence findings

Experimental groups	8-OHdG	GFAP
Control	20.15 ± 1.14^{a}	25.51 ± 1.11^{a}
ACR	81.12 ± 4.57^{b}	79.84 ± 3.98^{b}
MEL10+ACR	67.19 ± 4.15^{c}	57.15 ± 4.26^{c}
MEL20+ACR	35.84 ± 1.02^{d}	33.33 ± 2.11^{d}
MEL20	19.12 ± 1.83^{a}	26.48 ± 0.95^{a}

Different letters in the same column are statistically significant (a-b, a-c: $p < 0.01$; a-d, b-c, b-d, c-d: $p < 0.05$)

induced by the intraperitoneal administration of 50 mg/kg ACR for 14 days.

Regarding the locomotor activity, the animals in the ACR, MEL10+ACR, and MEL20+ACR groups exhibited skeletal muscle weakness, weight loss, and hind limb paralysis when compared with the control group. Although low-dose MEL administration slightly reversed the observed ACR-induced decrease in body weight, high-dose MEL (20 mg/kg) significantly reversed this decrease to the control value. Our findings corroborate previous research demonstrating that ACR-induced neurotoxicity in rat models leads to disrupted locomotor activity, impaired coordination, and suppressed weight gain [32]. ACR exposure causes dose-dependent damage to both central and peripheral nerves, resulting in disrupted gait scores including horizontal and vertical activities [33]. In our study, we also observed a significant decrease in locomotor activity (LMA) in the ACR toxicity group compared to the control group. However, the administration of MEL, particularly at high doses (20 mg/kg), had a protective effect against ACR-induced neurotoxicity, as evidenced by the higher LMA in the MEL group than in the ACR toxicity group, similar to the control group. Notably, the high dose of MEL did not affect vertical activity, possibly due to ACR-induced hind limb paralysis. Moreover, the high dose of MEL alone did not negatively impact the LMA.

The brain's heightened vulnerability to oxidative stress is intimately linked with the previous findings on locomotor activity. The brain's high metabolic rate, coupled with its limited cellular renewal capacity and abundance of polyunsaturated fatty acids, renders it particularly susceptible to the increase in ROS compared to other tissues [2, 8, 11]. In models of ACR-induced neurotoxicity, oxidative stress leads to an increase in MDA levels [34]. Previous study [35] has shown that MEL, a potent antioxidant and anti-inflammatory compound, protects brain tissue from damage by reducing MDA levels resulting from oxidative stress. In our study, we observed that 50 mg/kg ACR-induced neurotoxicity led to neuronal lipid peroxidation and subsequent increases in MDA levels. However, the administration of 20 mg/kg MEL significantly alleviated the ACR-induced increase in MDA levels. The cellular GSH pool also represents an important ROS scavenger that serves with GPx to prevent neuronal lipid peroxidation. ACR-induced oxidative stress depletes the cellular GSH reserve during biotransformation to its nontoxic analog, which markedly reduces GSH levels in brain tissue during ACR-induced neurotoxicity. Our findings align with these prior reports, demonstrating that ACR toxicity leads to reduced GSH levels in brain tissue due to oxidative stress. MEL mitigates oxidative stress through its antioxidant properties and elevates GSH levels [8–11]. Here, we observed a decrease in GSH levels in the ACR-exposed group, while administration of a high dose of MEL had antioxidant effects and prevented the ACR-induced reduction in GSH levels. SOD serves as the primary defense mechanism against superoxide radicals and acts as the frontline defense against oxidative stress.

Catalase (CAT) is another peroxisomal antioxidant enzyme that plays a crucial role in detoxifying harmful substances [36, 37]. CAT is among those antioxidant enzymes whose levels are significantly reduced after oxidative stress induced by ACR administration [11]. MEL, on the other hand, ameliorates oxidative stress and exerts neuroprotective effects against oxidative insult, which leads to decreases in SOD, GPx, and CAT activities [2]. In our study, treatment with a high dose of MEL rectified neuro-oxidative damage and decreased SOD, GPx, and CAT enzyme activity after the administration of 50 mg/kg ACR.

Moreover, in instances of neuroinflammation, microglia orchestrate defensive mechanisms within the brain, activating signaling pathways such as PI3K/AKT, MAPK, and mTOR in response to oxidative stress parameters [8]. This intricate cascade ultimately initiates NF-κB activation, underscoring the interconnectedness between oxidative stress and inflammation in neurological processes. This activation subsequently provokes the production of proinflammatory cytokines, chemokines, and inducible enzymes such as iNOS and COX-2, collectively contributing to the inflammatory response [38]. Notably, the pivotal proinflammatory cytokine TNF-α acts as a trigger for cytokine cascades associated with neuroinflammation while also regulating apoptosis [11, 39]. Conversely, MEL administration has demonstrated efficacy in reducing ACR-induced ROS production, inflammation, and

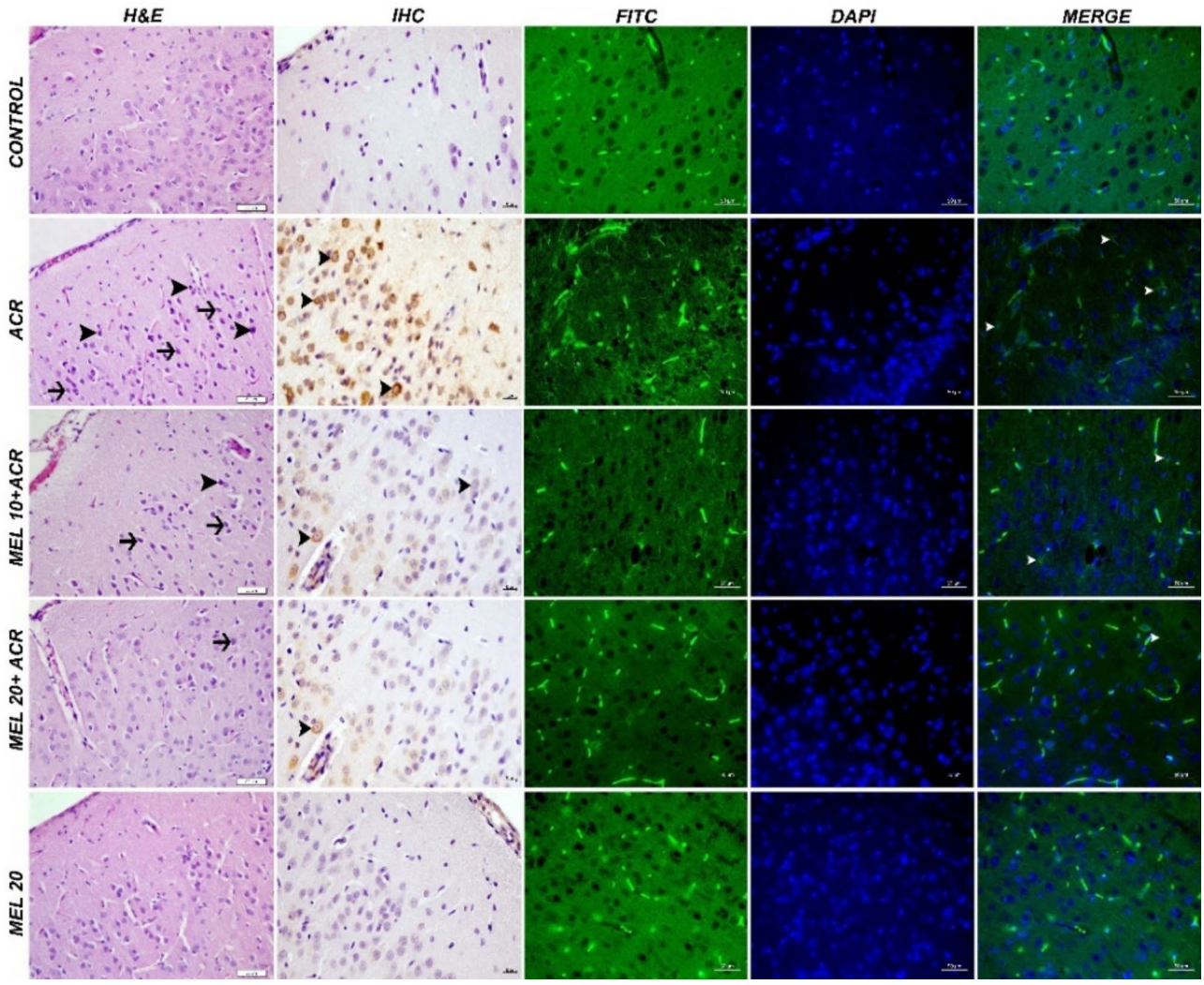

Fig. 5 Brain tissue, degeneration in neurons (arrows), necrosis in neurons (arrowheads), H&E, bar: 50 µm. Cytoplasmic 8-OHdG expressions in neurons (arrowheads), IHC-P, bar: 50 µm. GFAP expressions in astrocytes (FITC), IF, bar: 50 µm

mitochondrial damage, concurrently increasing antioxidant levels [26]. Our findings regarding ACR-induced inflammation and elevated TNF-α expression align with our previous finding, particularly at higher doses, exhibited potent anti-inflammatory effects by diminishing TNF-α levels. Furthermore, MEL administration effectively mitigates the increase in IL-1β levels during ACR toxic insult [8]. Similarly, our results revealed a notable increase in IL-1β levels in ACR-exposed rats compared to controls, while high doses of MEL (MEL20+ACR) successfully suppressed IL-1β expression, albeit with less efficacy observed with the lower MEL dose (MEL10+ACR).

ACR-induced neurotoxicity increases IL-6 levels [10]. Our study confirmed that ACR elevates IL-6 in brain tissue, while high-dose MEL prevents this increase. Nitric oxide (NO) is crucial for intercellular communication in the nervous system, regulating sleep, appetite, and neurotransmitter release. However, excessive NO production by nNOS forms reactive species like peroxynitrite and nitrotyrosine, leading to cell damage, neuronal death, and neurological disorders [40]. Increased nNOS activity triggers neuroinflammation, worsening neuronal damage [41]. Our investigation showed that elevated nNOS expression and neurotoxicity after 50 mg/kg ACR exposure, with high-dose MEL (MEL20+ACR) providing significant protection compared to low-dose MEL.

On the other hand, the AChE, a crucial enzyme at neuromuscular junctions and cholinergic synapses, is vital for memory and learning in the cerebral cortex. Elevated AChE activity, associated with cholinergic neuron damage and cognitive decline in conditions like diabetic neuropathy and neurodegenerative disorders with disrupted cell proliferation and accelerated apoptosis through oxidative damage [42]. Our study confirmed a significant rise in AChE activity in the ACR group compared to controls, with high-dose MEL (MEL20+ACR) effectively

reducing this increase, unlike the less effective low-dose MEL (MEL10+ACR). Similarly, epinephrine, norepinephrine, serotonin, and dopamine, essential monoamine neurotransmitters in various brain regions, are implicated in neurodegenerative diseases like Alzheimer's and Parkinson's. Increased MAO enzyme activity is a common finding in neurotoxicity models [43]. Our study showed elevated MAO levels in the ACR group, which high-dose MEL (MEL20+ACR) reduced to near-control levels, whereas low-dose MEL (MEL10+ACR) was less effective.

On cellular level, our study revealed that ACR induces ER in brain tissue, characterized by increased GRP78 gene expression. This stress arises from compromised ER functions, leading to the accumulation of misfolded proteins. Activation of UPR pathways, including PERK, ATF6, and IRE1, exacerbates cell viability reduction and apoptosis [44]. Specifically, ACR-induced ER stress triggers the PERK-eIF2α-ATF4 cascade, resulting in elevated CHOP expression and subsequent apoptosis. Our findings align with previous studies, indicating increased PERK activation, ATF4 expression, and GRP78 levels in response to ACR-induced ER stress [21].

Moreover, ACR-induced ER stress leads to the activation of the PERK-ATF6-IRE1 pathway, which plays a crucial role in apoptosis. This cascade activates CHOP, a marker of apoptosis, further regulating the expression of Bcl-2 and Bax, ultimately initiating apoptotic signaling [45]. Previous studies have shown that ACR-induced ER stress triggers CHOP-mediated apoptosis [46]. Our study confirms a significant increase in CHOP expression in the ACR-exposed group.

Remarkably, MEL administration dose-dependently suppressed the increase in CHOP expression, indicating its potential to alleviate ACR-induced apoptosis mediated by ER stress. Additionally, we observed elevated ATF6 and sXBP1 gene expression due to neuronal ER stress, which was effectively mitigated by dose-dependent MEL administration. This underscores MEL's potential to modulate ER stress-related pathways and protect against neurotoxicity induced by ACR.

ACR-induced ER stress leads to downregulation of Bcl-2 expression and overexpression of Bax and Caspase-3, promoting apoptosis. In our study, ACR exposure suppressed Bcl-2 gene expression while increasing Bax and Caspase-3 levels that result in neuronal apoptosis. This meets with previous findings where ACR-induced ER stress activates the PERK-eIF2α-ATF4 pathway, elevating CHOP expression and triggering apoptosis [44]. MEL administration demonstrated dose-dependent neuroprotective effects by preventing declines in Bcl-2 levels and increases in Bax and Caspase-3 levels. Specifically, in rats exposed to ACR, MEL treatment increased Bcl-2 expression and decreased Bax and Caspase-3 levels, mitigating CHOP-mediated apoptosis [45]. This suggests MEL's potential to alleviate ACR-induced apoptosis through modulation of ER stress-related pathways [46–50].

Furthermore, the activation of apoptosis pathways reduces Bcl-2 expression and boosts Bax levels, ultimately increasing Caspase-3 activity. Our findings are consistent with other studies that demonstrated MEL's impact on ER stress-induced apoptosis, showing its ability to modulate key apoptotic markers and protect neuronal cells from ACR-induced damage [51, 52].

Our study reveals significant degenerative disorders in ACR-exposed rat brains, consistent with previous models of ACR-induced neurotoxicity [35]. However, treatment with MEL effectively prevented these pathologies. Notably, brain sections from ACR-exposed rats exhibited severe neuronal degeneration and necrosis, accompanied by pronounced vessel hyperemia. Interestingly, low-dose MEL partially attenuated ACR-induced damage, while high-dose MEL robustly prevented significant degeneration and maintained mild hyperemia.

The oxidative stress, fueled by ROS, disrupts cellular structures, leading to increased 8-OHdG expression, a marker of oxidative DNA damage in ACR-exposed rat brains. Here our immunohistochemical findings confirm this elevation. Remarkably, dose-dependent MEL application significantly countered this increase, offering substantial protection against ACR-induced neurotoxicity.

Moreover, astrocytes play a crucial role in maintaining brain structure, with GFAP being a primary intermediate filament [53]. Elevated GFAP levels are indicative of brain injury and degeneration, as seen in ACR-exposed rat brains [54], the immunofluorescence results corroborate previous reports, highlighting increased GFAP expression. Remarkably, MEL's dose-dependent administration effectively mitigated GFAP elevation, underscoring its potential as a neuroprotective agent.

Conclusion

In conclusion, ACR poses significant neurological risks due to its diverse toxic effects, including neurotoxicity and oxidative stress. Our study in a rat model revealed ACR-induced hind limb paralysis, muscle weakness, weight loss, and impaired locomotor activity, as well as evidence of oxidative damage and reduced antioxidant enzyme activity in brain tissue. Treatment with MEL, a potent antioxidant, mitigated oxidative stress, restored antioxidant enzyme levels, and suppressed neuroinflammation by reducing proinflammatory cytokine expression. Moreover, MEL prevented apoptosis by modulating the expression of apoptosis-related genes and preserving neuronal integrity. These findings highlight the neuroprotective potential of MEL against ACR-induced neurotoxicity and underscore its therapeutic relevance in

mitigating neurotoxic insults. Further research is needed to elucidate the precise mechanisms underlying the protective effects of MEL and optimize its therapeutic neuroprotective effects.

Acknowledgements
This work was fully supported by Atatürk University Scientific Research fund.

Author contributions
YD: Methodology, analysis, writing. SY: Analysis, writing. ES: Analysis, writing. FA: Analysis. MG: Analysis. AC: Method planning, analysis, writing, final revision of the manuscript.

Funding
This study was supported by the Atatürk University Scientific Research Projects Coordinator (Project No: 2020/8687). Therefore, we are grateful to Atatürk University, Turkey.

Data availability
No datasets were generated or analysed during the current study.

Declarations

Ethics approval and consent to participate
The research was approved by the Atatürk University Ethical Committee for laboratory animal experiments (Ethics Committee Protocol number: 2020/41). All experiments were performed in strict accordance with the ARRIVE guidelines and all relevant institutional and national regulations for the care and use of laboratory animals. Additionally, all methods were carried out in compliance with the guidelines and regulations specified by the Biomed Central ethical policies.

Consent for publication
The authors give their consent for the publication of identifiable details, including the images within the text to be published in the journal and article.

Competing interests
The authors declare no competing interests.

Author details
[1]Department of Physiology, Faculty of Veterinary Medicine, Atatürk University, Erzurum, Turkey
[2]Department of Pathology, Faculty of Veterinary Medicine, Atatürk University, Erzurum, Turkey
[3]Department of Pathology, Faculty of Veterinary Medicine, Kyrgyzstan-Turkey Manas University, Bishkek, Kyrgyzstan
[4]Department of Pharmacology, Faculty of Medicine, Atatürk University, Erzurum, Turkey

Received: 24 October 2024 / Accepted: 7 March 2025
Published online: 11 March 2025

References

1. Yan F, Wang L, Zhao L, Wang C, Lu Q, Liu R. Acrylamide in food: occurrence, metabolism, molecular toxicity mechanism and detoxification by phytochemicals. Food Chem Toxicol. 2023;175:113696.
2. Yildirim S, Sengul E, Aksu EH, Cinar İ, Gelen V, Tekin S, et al. Selenium reduces acrylamide-induced testicular toxicity in rats by regulating HSD17B1, star, and CYP17A1 expression, oxidative stress, inflammation, apoptosis, autophagy, and DNA damage. Environ Toxicol Pharmacol. 2024;39(3):1402–14.
3. Iyer AM, Dadlani V, Pawar HA. Review on acrylamide: a hidden hazard in fried carbohydrate-rich food. Curr Nutr Food Sci. 2022;18:274–86.
4. Hogervorst JG, Saenen ND, Nawrot TS. Gestational acrylamide exposure and biomarkers of fetal growth: probing the mechanism underlying the association between acrylamide and reduced fetal growth. Environ Int. 2021;155:106668.
5. Bellicha A, Wendeu-Foyet G, Coumoul X, Koual M, Pierre F, Guéraud F, et al. Dietary exposure to acrylamide and breast cancer risk: results from the NutriNet-Santé cohort. Am J Clin Nutr. 2022;116:911–9.
6. Filippini T, Halldorsson TI, Capitão C, Martins R, Giannakou K, Hogervorst J, et al. Dietary acrylamide exposure and risk of site-specific cancer: a systematic review and dose-response meta-analysis of epidemiological studies. Front Nutr. 2022;9:875607.
7. Ikeda S, Sobue T, Kitamura T, Ishihara J, Kotemori A, Zha L, et al. Dietary acrylamide intake and the risks of renal cell, prostate, and bladder cancers: a Japan public health center-based prospective study. Nutr. 2021;13:780.
8. Ibaokurgil F, Aydin H, Yildirim S, Sengul E. Melatonin alleviates oxidative stress, inflammation, apoptosis, and DNA damage in acrylamide–induced nephrotoxicity in rats. Asian Pac J Trop Biomed. 2023;13:121–30.
9. Gelen V, Yıldırım S, Şengül E, Çınar A, Çelebi F, Küçükkalem M, et al. Naringin attenuates oxidative stress, inflammation, apoptosis, and oxidative DNA damage in acrylamide-induced nephrotoxicity in rats. Asian Pac J Trop Biomed. 2022;12:223–32.
10. Sengul E, Gelen V, Yildirim S, Tekin S, Dag Y. The effects of selenium in acrylamide-induced nephrotoxicity in rats: roles of oxidative stress, inflammation, apoptosis, and DNA damage. Biol Trace Elem Res. 2021;199:173–84.
11. Sengul E, Gelen V, Yildirim S, Cinar İ, Aksu EH. Effects of naringin on oxidative stress, inflammation, some reproductive parameters, and apoptosis in acrylamide-induced testis toxicity in rat. Envir Toxicol Pharmacol. 2023;38:798–808.
12. Bin-Jumah M, Abdel-Fattah A-FM, Saied EM, El-Seedi HR, Abdel-Daim MM. Acrylamide-induced peripheral neuropathy: manifestations, mechanisms, and potential treatment modalities. Environ Sci Pollut Res. 2021;28:13031–46.
13. Zhang P, Pan H, Wang J, Liu X, Hu X. Telomerase activity-independent function of telomerase reverse transcriptase is involved in acrylamide-induced neuron damage. Biotech Histochem. 2014;89:327–35.
14. Sloan SA, Barres BA. Mechanisms of astrocyte development and their contributions to neurodevelopmental disorders. Curr Opin Neurobiol. 2014;27:75–81.
15. LoPachin RM, Gavin T. Molecular mechanism of acrylamide neurotoxicity: lessons learned from organic chemistry. Environ Health Perspect. 2012;120:1650–7.
16. Sarkar R, Rao KBN, Jha MP, Mapa K. Endoplasmic reticulum-unfolded protein response pathway modulates the cellular response to mitochondrial proteotoxic stress. Cell Stress Chaperon. 2022;27:241–56.
17. Yuan S, She D, Jiang S, Deng N, Peng J, Ma L. Endoplasmic reticulum stress and therapeutic strategies in metabolic, neurodegenerative diseases and cancer. Mol Med. 2024;30:40.
18. Hasan S-A-M, James AW, Fazili FM, Tarabishi S, Sheikh NM, Shah ZA. Endoplasmic reticulum stress in neurodegenerative diseases. J Alzheimer's Dis. 2024;1:87–97.
19. Tabas I, Ron D. Integrating the mechanisms of apoptosis induced by Endoplasmic reticulum stress. Nat Cell Biol. 2011;13:184–90.
20. Xia Q, Feng X, Huang H, Du L, Yang X, Wang K. Gadolinium-induced oxidative stress triggers Endoplasmic reticulum stress in rat cortical neurons. J Neurochem. 2011;117:38–47.
21. Komoike Y, Matsuoka M. Endoplasmic reticulum stress-mediated neuronal apoptosis by acrylamide exposure. Toxicol Appl Pharmacol. 2016;310:68–77.
22. Zargar S, Siddiqi NJ, Ansar S, Alsulaimani MS, El Ansary AK. Therapeutic role of Quercetin on oxidative damage induced by acrylamide in rat brain. Pharm Biol. 2016;54:1763–7.
23. Lee JG, Woo YS, Park SW, Seog D-H, Seo MK, Bahk W-M. The neuroprotective effects of melatonin: possible role in the pathophysiology of neuropsychiatric disease. Brain Sci. 2019;9:285.
24. Muñoz-Jurado A, Escribano BM, Caballero-Villarraso J, Galván A, Agüera E, Santamaría A, et al. Melatonin and multiple sclerosis: antioxidant, anti-inflammatory and immunomodulator mechanism of action. Inflammopharmacology. 2022;30:1569–96.
25. Tozihi M, Shademan B, Yousefi H, Avci CB, Nourazarian A, Dehghan G. Melatonin: a promising neuroprotective agent for cerebral ischemia-reperfusion injury. Front Aging Neurosci. 2023;15:1227513.
26. Edres HA, Taha NM, Lebda MA, Elfeky MS. The potential neuroprotective effect of allicin and melatonin in acrylamide-induced brain damage in rats. Environ Sci Pollut Res. 2021;28:58768–80.
27. Ozturk I, Elbe H, Bicer Y, Karayakali M, Onal MO, Altinoz E. Therapeutic role of melatonin on acrylamide-induced hepatotoxicity in pinealectomized rats: effects on oxidative stress, NF-κB signaling pathway, and hepatocellular proliferation. Food Chem Toxicol. 2023;174:113658.

28. Pan X, Zhu L, Lu H, Wang D, Lu Q, Yan H. Melatonin attenuates oxidative damage induced by acrylamide in vitro and in vivo. Oxid Med Cell Longev. 2015;2015:703709.
29. Kraeuter A-K, Guest PC, Sarnyai Z. The open field test for measuring locomotor activity and anxiety-like behavior. Pre-Clinical Models Tech Protocols. 2019:99–103.
30. Xu Z, Qian B. Sevoflurane anesthesia-mediated oxidative stress and cognitive impairment in hippocampal neurons of old rats can be ameliorated by expression of brain derived neurotrophic factor. Neurosci Lett. 2020;721:134785.
31. Marković Filipović J, Miler M, Kojić D, Karan J, Ivelja I, Čukuranović Kokoris J, et al. Effect of acrylamide treatment on Cyp2e1 expression and redox status in rat hepatocytes. Int J Mol Sci. 2022;23:6062.
32. Goudarzi M, Mombeini MA, Fatemi I, Aminzadeh A, Kalantari H, Nesari A, et al. Neuroprotective effects of ellagic acid against acrylamide-induced neurotoxicity in rats. Neurol Res. 2019;41:419–28.
33. Su B, Guan Q, Wang M, Liu N, Wei X, Wang S, et al. Calpeptin is neuroprotective against acrylamide-induced neuropathy in rats. Toxicol Appl Pharmacol. 2018;400:1–8.
34. Acaroz U, Ince S, Arslan-Acaroz D, Gurler Z, Kucukkurt I, Demirel HH, et al. The ameliorative effects of Boron against acrylamide-induced oxidative stress, inflammatory response, and metabolic changes in rats. Food Chem Toxicol. 2018;118:745–52.
35. Sokolovic D, Djindjic B, Nikolic J, Bjelakovic G, Pavlovic D, Kocic G, et al. Melatonin reduces oxidative stress induced by chronic exposure of microwave radiation from mobile phones in rat brain. J Radiat Res. 2008;49:579–86.
36. Glorieux C, Calderon PB. Catalase, a remarkable enzyme: targeting the oldest antioxidant enzyme to find a new cancer treatment approach. Biol Chem. 2017;398:1095–108.
37. Tekin S, Sengul E, Yildirim S, Aksu EH, Bolat İ, Çınar B, et al. Molecular insights into the antioxidative and anti-inflammatory effects of P-coumaric acid against bisphenol A-induced testicular injury: in vivo and in Silico studies. Reprod Toxicol. 2024;125:108579.
38. Yue B, Ren Y-J, Zhang J-J, Luo X-P, Yu Z-L, Ren G-Y, et al. Anti-inflammatory effects of Fargesin on chemically induced inflammatory bowel disease in mice. Molecules. 2018;23:1380.
39. Sengul E, Yildirim S, Cinar İ, Tekin S, Dag Y, Bolat M et al. Mitigation of acute hepatotoxicity induced by cadmium through Morin: modulation of oxidative and pro-apoptotic Endoplasmic reticulum stress and inflammatory responses in rats. Biol Trace Elem Res. 2024:1–12.
40. Arami KM, Jameie B, Moosavi SA. Neuronal nitric oxide synthase. Nitric oxide synthase: simple enzyme-complex roles. 2017; 1.
41. Palus K, Makowska K, Całka J. Alterations in galanin-like immunoreactivity in the enteric nervous system of the Porcine stomach following acrylamide supplementation. Int J Mol Sci. 2019;20:3345.
42. Chavda V, Yadav D, Patel S, Song M. Effects of a diabetic microenvironment on neurodegeneration: special focus on neurological cells. Brain Sci. 2024;14:284.
43. Özdemir Z, Alagöz MA, Bahçecioğlu ÖF, Gök S. Monoamine oxidase-B (MAO-B) inhibitors in the treatment of Alzheimer's and Parkinson's disease. Curr Med Chem. 2021;28:6045–65.
44. Singh R, Kaur N, Choubey V, Dhingra N, Kaur T. Endoplasmic reticulum stress and its role in various neurodegenerative diseases. Brain Res. 2023:148742.
45. Li Y, Guo Y, Tang J, Jiang J, Chen Z. New insights into the roles of CHOP-induced apoptosis in ER stress. Acta Biochim Biophys Sin. 2014;46:629–40.
46. Wang Y, Duan L, Zhang X, Jiao Y, Liu Y, Dai L, et al. Effect of long-term exposure to acrylamide on endoplasmic reticulum stress and autophagy in rat cerebellum. Ecotoxicol Environ Saf. 2021;224:112691.
47. Erfan OS, Sonpol HM, Abd El-kader M. Protective effect of rapamycin against acrylamide-induced hepatotoxicity: the associations between autophagy, apoptosis, and necroptosis. Anat Rec. 2021;304:1984–98.
48. Liu Y, Zhao H, Yin K, Guo M, Wang Y, Wang D, et al. The protective effect of Zn2 + on As3 + toxicity in common carp: resistance to oxidative stress, inhibition of endoplasmic reticulum stress, apoptosis and autophagy. Aquaculture. 2022;546:737375.
49. Gelen V, Şengül E, Yıldırım S, Senturk E, Tekin S, Kükürt A. The protective effects of hesperidin and curcumin on 5-fluorouracil–induced nephrotoxicity in mice. Environ Sci Pollut Res. 2021;28:47046–55.
50. Tekin S, Çelebi F. Investigation of the effect of hesperidin on some reproductive parameters in testicular toxicity induced by B isphenol A. Andrologia. 2022;54:e14562.
51. Wang W, Huang L, Hu Y, Thomas E, Li X. Neuroprotective effects of notoginsenoside R1 by upregulating Trx-1 on acrylamide-induced neurotoxicity in PC12. Hum Exp Toxicol. 2020;39:797–807.
52. Fan C, Feng J, Tang C, Zhang Z, Feng Y, Duan W, et al. Melatonin suppresses ER stress-dependent proapoptotic effects via AMPK in bone mesenchymal stem cells during mitochondrial oxidative damage. Stem Cell Res Therapy. 2020;11:1–22.
53. Middeldorp J, Hol E. GFAP in health and disease. Prog Neurobiol. 2011;93:421–43.
54. Farag OM, Abd-Elsalam RM, Ogaly HA, Ali SE, El Badawy SA, Alsherbiny MA, et al. Metabolomic profiling and neuroprotective effects of purslane seeds extract against acrylamide toxicity in rat's brain. Neurochem Res. 2021;46:819–42.

Publisher's note